Volume 6 | Number 8 | 21 April 2014 | Pages 3897–4396

Nanoscale

www.rsc.org/nanoscale

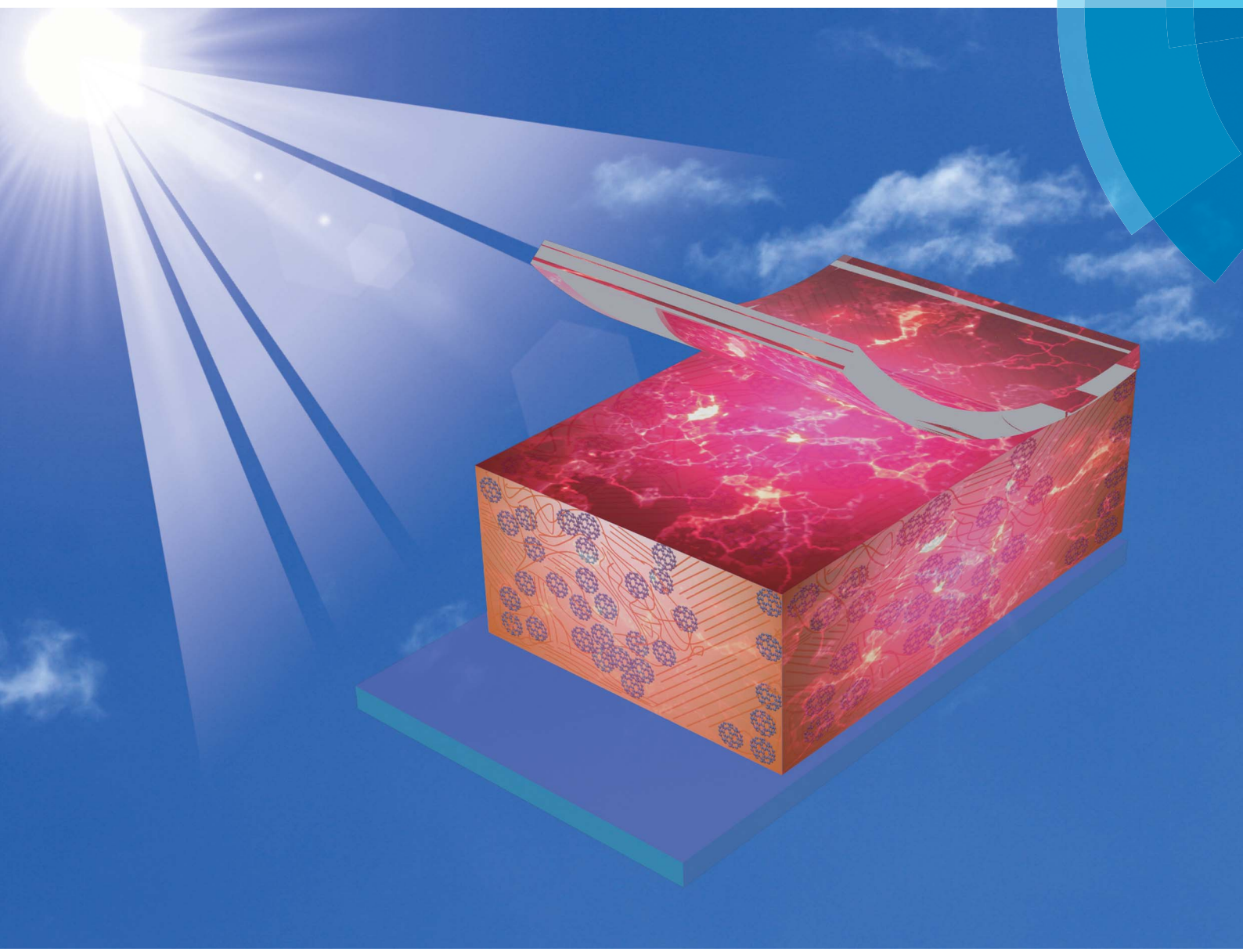

ISSN 2040-3364

ROYAL SOCIETY OF CHEMISTRY

REVIEW ARTICLE

Lin *et al.*

Optimization of molecular organization and nanoscale morphology for high performance low bandgap polymer solar cells

NCNST

Nanoscale

REVIEW

View Article Online
View Journal | View Issue

Cite this: *Nanoscale*, 2014, **6**, 3984

Optimization of molecular organization and nanoscale morphology for high performance low bandgap polymer solar cells

Ming He,[a] Mengye Wang,[ab] Changjian Lin[b] and Zhiqun Lin*[a]

Received 27th November 2013
Accepted 18th December 2013

DOI: 10.1039/c3nr06298h

www.rsc.org/nanoscale

Rational design and synthesis of low bandgap (LBG) polymers with judiciously tailored HOMO and LUMO levels have emerged as a viable route to high performance polymer solar cells with power conversion efficiencies (PCEs) exceeding 10%. In addition to engineering the energy-level of LBG polymers, the photovoltaic performance of LBG polymer-based solar cells also relies on the device architecture, in particular the fine morphology of the photoactive layer. The nanoscale interpenetrating networks composed of nanostructured donor and acceptor phases are the key to providing a large donor–acceptor interfacial area for maximizing the exciton dissociation and offering a continuous pathway for charge transport. In this Review Article, we summarize recent strategies for tuning the molecular organization and nanoscale morphology toward an enhanced photovoltaic performance of LBG polymer-based solar cells.

1. Introduction

Polymer-based photovoltaics hold the promise for light-weight, large area and high performance solar cells through low cost roll-to-roll processing.[1–7] A typical polymer solar cell consists of conjugated polymer (CP) donor and fullerene acceptor materials, in which regioregular poly(3-hexylthiophene) (P3HT) is often exploited as a prototype donor material because of its good light absorption, strong π–π interaction, and facile synthesis,[8–12] and fullerene derivatives (*e.g.*, [6,6]-phenyl-C_{61}-butyric acid methyl ester ($PC_{61}BM$), [6,6]-phenyl-C_{71}-butyric acid methyl ester ($PC_{71}BM$), and indene-C_{60} bisadduct (ICBA)) are employed as acceptor materials due to their strong electron affinity, high electron mobility, and ultrafast charge transfer.[5,13,14] Owing to the nature of weak electronic interactions between organic molecules and the low dielectric constant of CPs, electron–hole pairs (*i.e.*, excitons) generated in CP donors by the absorption of photons are strongly bound by Coulombic force.[15] These photogenerated excitons must diffuse toward the donor–acceptor interface and relax to the charge transfer (CT) exciton state driven by the energy offset between the lowest unoccupied molecular orbital (LUMO) levels of donor and

[a]*School of Materials Science and Engineering, Georgia Institute of Technology, Atlanta, GA 30332, USA. E-mail: zhiqun.lin@mse.gatech.edu*

[b]*Department of Chemistry, College of Chemistry and Chemical Engineering, Xiamen University, Xiamen 361005, China*

Ming He received his Ph.D. degree in Polymer Chemistry and Physics from Fudan University of China in 2011. Currently, he works as a postdoctoral fellow in Professor Zhiqun Lin's research group at Georgia Institute of Technology. His research interests include conjugated polymers, block copolymers, quantum dots, polymer solar cells, dye-sensitized solar cells, graphene electrode materials, and thermoelectrical nanocomposites.

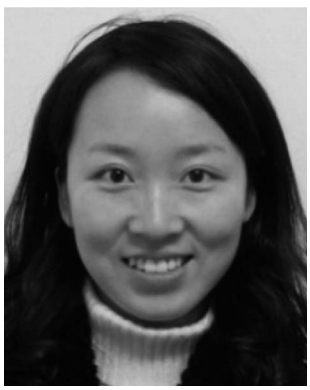

Mengye Wang is a Ph.D. student in the College of Chemistry and Chemical Engineering at Xiamen University. She received her Bachelor of Science in Chemistry from Xiamen University in 2010. She is currently a visiting PhD student in Prof. Zhiqun Lin's group at Georgia Institute of Technology. Her research interests include the applications of TiO_2 in photocatalytic degradation of organic pollutants, water splitting, dye-sensitized solar cells, and polymer solar cells.

acceptor materials.[16–18] The vibrational energy released due to the formation of CT excitons acts as the external energy to completely dissociate the CT excitons into free charge carries if it exceeds the binding energy of excitons.[18] These free charge carries are then transported to and collected on the respective electrodes.

In this context, the power conventional efficiency (PCE) of polymer solar cells depends on both intrinsic energy-level alignment and extrinsic architecture of donor–acceptor blends.[19,20] For the energy-level alignment, the optical bandgap (E_g) of CP donors ranging from ~1.2 to ~1.9 eV is preferred for absorbing visible and near-infrared sunlight to increase the short-circuit current density (J_{sc}),[21] which can be realized by moving upward the highest occupied molecular orbital (HOMO) level or downward the LUMO level of CP donors. However, a grand challenge is that the LUMO level of CP donors is supposed to align at least 0.3 eV higher than that of fullerene acceptors to ensure the dissociation of excitons at the donor–acceptor interface, meanwhile the HOMO level of CP donors needs to move far away from the LUMO level of fullerene acceptors to maximize the open voltage (V_{oc}).[21–23] Clearly, the energy levels of CP donors need to be delicately tuned to simultaneously broaden the absorption and increase the V_{oc}.

Recent development in "push–pull" alternating low bandgap (LBG) polymers renders the energy-level engineering of CP donors by adjusting the intramolecular charge transfer (ICT) between the electron-donating (*i.e.*, to push electron) units and the electron-withdrawing (*i.e.*, to pull electron) units,[24–27] leading to low optical bandgaps, tunable HOMO/LUMO levels, and ultimately enhanced photovoltaic performance. In particular, the electron-withdrawing unit enables the LUMO level of CP donors to move downward further than the HOMO level, corresponding to an lowered bandgap of CP donors as well as an increased energy offset between the HOMO level of CP donors and the LUMO level of fullerene acceptors.[28] The reduction of CP bandgap can also be achieved by incorporating rigid fused aromatic structures into the conjugated backbones. Such an incorporation increases the planarity of CP chains, promotes the delocalization of π-electrons, and thus improves the charge carrier mobility.[29] Based on the principle of energy-level engineering noted above, a variety of LBG polymer donors have been synthesized.[30–34] For example, the "push–pull" polymer (PBnDT-DTffBT, Fig. 1a) composed of 5,6-difluoro-4,7-dithien-2-yl-2,1,3-benzothiadiazole (DTffBT) as the electron-withdrawing unit and benzo[1,2-*b*:4,5-*b*′]dithiophene (BnDT) as the electron-donating unit exhibited a deeply-lying HOMO level of −5.54 eV as compared to that of −4.76 eV in P3HT,[35,36] a reduced bandgap of 1.7 eV as compared to that of 1.9 eV in P3HT,[8] and a high PCE of 7.2% with a V_{oc} of 0.91 V, a J_{sc} of 12.9 mA cm^{-2}, and a fill factor (FF) of 61.2%.[35] Recently, the PCEs of LBG polymer-based solar cells have exceeded 10% in the tandem solar cells based on poly[2,7-(5,5-bis-(3,7-dimethyloctyl)-5*H*-dithieno [3,2-*b*:2′,3′-*d*′]pyran)-*alt*-4,7-(5,6-difluoro-2,1,3-benzothia diazole)] (PDTP-DFBT, Fig. 1b) and P3HT.[37] The LBG polymer PDTP-DFBT possesses a bandgap of 1.38 eV, a hole mobility of 3.2×10^{-3} cm^2 V^{-1} s^{-1} and a HOMO level of −5.26 eV. As a result, a PDTP-DFBT-based single-junction device had a high external quantum efficiency (EQE) over 60% and a spectral response from 300 nm to 900 nm.[37]

Besides the energy-level engineering, the performance of polymer solar cells is also determined by the device architecture,[38–40] in particular the film morphology of the photoactive layer, due to the intrinsically short exciton diffusion length (*i.e.*, 5–20 nm) of CPs.[16] The bulk heterojunction (BHJ) has been widely recognized as the most advantageous architecture for high performance polymer solar cells.[41] In a BHJ cell the interpenetration of nanostructured donor–acceptor domains provides not only a large donor–acceptor interface area for maximizing the exciton dissociation, but also a continuous charge transport pathway to facilitate the dissociated electrons and holes to move toward the respective electrodes with minimized charge carrier recombination.[42,43] It is noteworthy that the molecular packing of CPs within the BHJ structure profoundly influences the resulting optoelectronic properties. It

Changjian Lin is a Professor in the State Key Laboratory of Physical Chemistry of Solid Surfaces, and College of Chemistry and Chemical Engineering at Xiamen University. He received his Ph.D. in Physical Chemistry from Xiamen University in 1985. His research interests include electrochemical methods, corrosion and protection, biomaterials and biosurfaces, advanced materials for energies and environments, such as dye-sensitized and quantum dot-sensitized solar cells, photogenerated cathodic protection, surface wettability, water splitting hydrogen production and photocatalytic degradation of organic pollutants.

Zhiqun Lin is an Associate Professor in the School of Materials Science and Engineering at Georgia Institute of Technology. He received his Ph.D. in Polymer Science and Engineering from University of Massachusetts, Amherst in 2002. His research interests include polymer solar cells, dye-sensitized solar cells, semiconductor organic–inorganic nanocomposites, photocatalysis, quantum dots (rods), conjugated polymers, block copolymers, polymer blends, hierarchical structure formation and assembly, surface and interfacial properties, multifunctional nanocrystals, and Janus nanostructures. He is a recipient of an NSF Career Award.

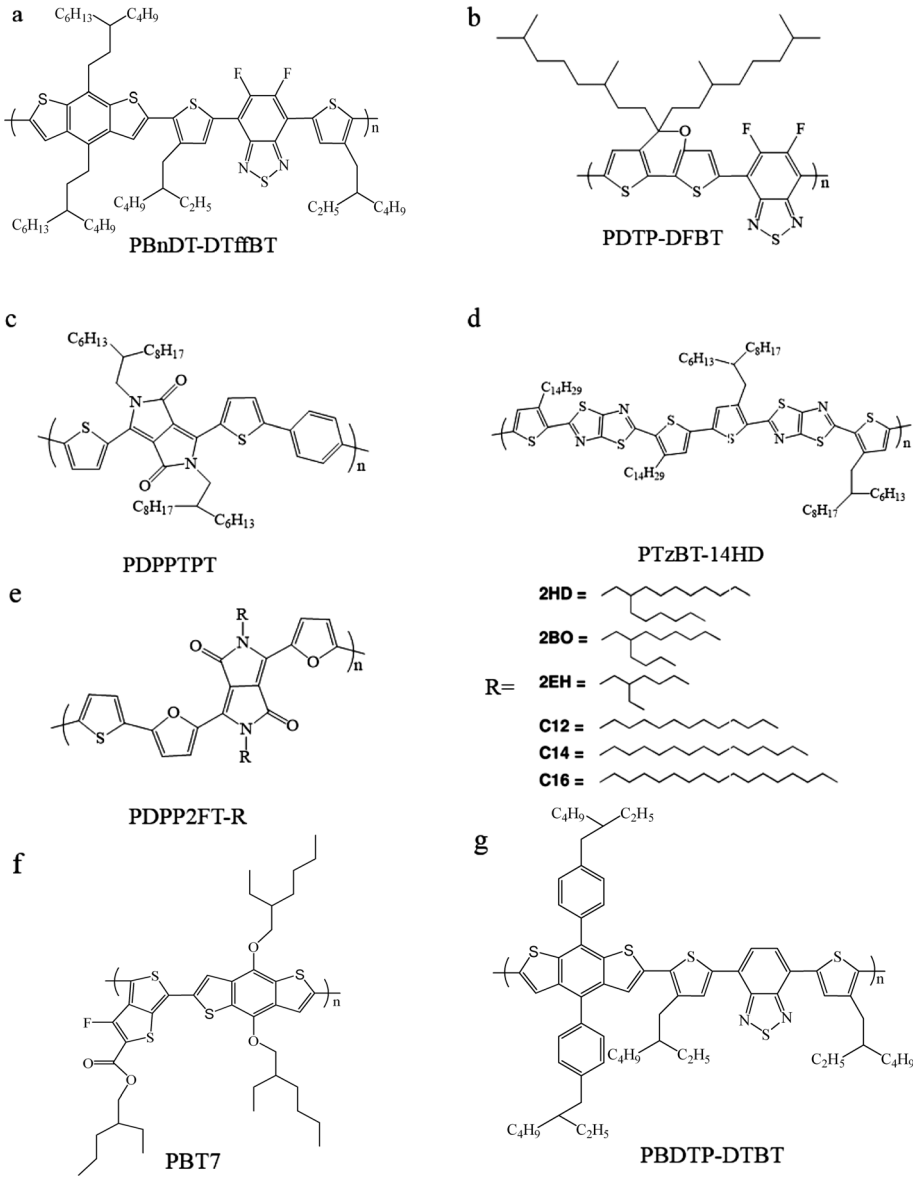

Fig. 1 Molecular structures of typical LBG polymers.

leads to (1) an increased π–π stacking that facilitates the anisotropic π-orbital delocalization along the conjugated backbones,[44] which is beneficial for broadening the light absorption and increasing the charge carrier mobility;[45] and (2) a preferential alignment of π–π stacking perpendicular to the substrate (*i.e.*, face-on orientation) that further improves the charge carrier transport to the respective electrodes.[46,47] Studies on the correlation between the film morphology and the photovoltaic performance of polymer solar cells have been focused on conventional conjugated homopolymer-based solar cells (*e.g.*, poly[2-methoxy-5-(2′-ethyl-hexyloxy)-1,4-phenylene vinylene] (MEH-PPV), poly[2-methoxy-5-(3′,7′-dimethyloctyloxy)-1,4-phenylene vinylene] (MDMO-PPV), and P3HT) using the state-of-the-art characterization techniques such as transmission electron microscopy (TEM), scanning electron microscopy (SEM), scanning tunneling microscopy (STM), Raman microscopy, photoconductive atomic force microscopy (p-AFM), grazing incidence small angle X-ray scattering (GISAXS), grazing incidence wide angle X-ray diffraction (GIWAXD), resonant soft X-ray scattering (RSoXS), and small angle neutron scattering (SANS).[48–54] To date, much progress has been made in the understanding of the morphology-dominated device efficiency; the photovoltaic performance of conjugated homopolymer-based solar cells can be optimized through adjusting the solvents used, thicknesses of the active layer, film deposition methods, compositions of the interfacial layer, and post-treatment procedures to allow a better control over the film morphology.[55–60]

In contrast, research on LBG polymer-based solar cells is still centered on the design of new molecular structures with suitable energy levels. Considering the complicated molecular structures, the relationship between the film morphology and

optoelectronic properties of LBG polymers is far less understood in comparison with that of conjugated homopolymers. Compared to the semicrystalline nature of P3HT, LBG polymers often possess a poor crystallinity and some of them are even amorphous due to the large steric constrains of complex molecular structures. The thermal- and solvent-annealing treatments, the widely used post-treatment procedures for conjugated homopolymer-based solar cells,[61–63] appear ineffective in optimizing the film morphology of LBG polymer-based solar cells. Nevertheless, the use of solvent additives works prominently in improving the photovoltaic performance of LBG polymers.[64,65] The non-covalent interactions of "push–pull" units (*e.g.*, aromatic π–π interaction, intramolecular chalcogen–chalcogen interaction, hydrogen bonding, *etc.*) play a crucial role in molecular organization, film morphology, and ultimately optoelectronic properties of LBG polymers.[66,67] This Review Article seeks to highlight recent strategies for tuning the molecular organization and nanoscale morphology toward an enhanced photovoltaic performance of LBG polymer-based solar cells. We make no attempt to thoroughly cover the literature of CP-based solar cells here but refer the reader to some comprehensive reviews.[68–71]

2. Molecular engineering for optimized morphology

2.1 Controlling the molecular weight

The kinetics of the formation of BHJ structures are such that the degree of crystallization and polymer/fullerene microphase separation can be controlled by several extrinsic and intrinsic factors. The extrinsic factors are related to the film-processing, including the processing solvent, film-deposition method, and post-treatment procedure,[72] and the intrinsic factors concern the molecular properties of CPs, such as the molecular weight (MW), conjugated length, and the solubilization of side chains.[11,73] The MW is a key factor that affects the crystallization and phase behavior of CPs.[74] A CP with high MW is preferred for generating locally aligned molecular packing with few structure defects,[75] thereby providing long pathways for charge transport with few trap sites,[76] building better connections between crystalline domains with few grain boundaries,[77] and thus leading to enhanced optoelectronic properties. It is worth noting that, however, CPs with ultrahigh MW should be avoided. This can be attributed to the fact that an ultrahigh MW CP would commonly generate a high level of structural disorder,[78] poor solubility in processing solvents, and low miscibility with donor materials.[74]

Due to complex molecular structures, it is often difficult to achieve a LBG polymer with high MW. Diketopyrrolopyrrole (DPP) has been widely employed as a promising electron-withdrawing unit for LBG polymers.[79] The MW of the DPP-based LBG polymer PDPPTPT (Fig. 1c) can be controlled *via* changing the amount of $Pd_2(dba)_3$/PPh_3 catalyst in the Suzuki polymerization of DPP and thiophene–phenylene–thiophene units.[80] It has been demonstrated that for a low MW PDPPTPT (M_n = 10 kg mol^{-1}), the resulting PDPPTPT-based solar cell showed a high V_{oc} of 0.80 V; however, the PCE only reached 5.5% with a relatively low J_{sc} of 10.8 mA cm^{-2}.[80] Through adjusting the amount of Pd catalyst, the MW of PDPPTPT was increased to M_n = 72 kg mol^{-1}, and the PCEs based on the high MW PDPPTPT were raised to 7.4% accompanied by an increase of J_{sc} from 10.8 mA cm^{-2} to 14 mA cm^{-2}.[81] As the HOMO level and bandgap of the as-synthesized high MW PDPPTPT were comparable with those of the low MW counterpart, the improved efficiency was closely correlated with the appearance of finer-dispersed PDPPTPT nanofibers within the high MW PDPPTPT/$PC_{71}BM$ blends.[81,82] This result indicated an enhanced crystallization of high MW PDPPTPT that intermixed with $PC_{71}BM$, leading to an improved exciton dissociation and charge transport.

In addition to the enhancement of crystallization, the preferred molecular orientation of LBG polymers is also affected by MW, which is associated with the self-assembly tendency of LBG polymers and fullerene molecules, and the intermolecular interactions between them.[74] Recently, the thiazolothiazole-based LBG polymer PTzBT-14HD (Fig. 1d) with a series of different MWs (M_n = 13 kg mol^{-1}, 20 kg mol^{-1}, 33 kg mol^{-1}, and 73 kg mol^{-1}) was synthesized by varying the monomer purity using repeated recrystallizations.[83] The PTzBT-14HD thin films exhibited an increasing trend to have the edge-on orientation as the MW increased. Based on the 2D GIWXRD patterns of PTzBT-14HD thin films, the scattering vector q of 0.2–0.3 Å^{-1} on the q_z axis can be attributed to the lamellar-packing diffraction, while the vector q of 1.7 Å^{-1} on the q_{xy} axis originates from the π–π stacking diffraction (Fig. 2a–d).[83–85] More intriguingly, the PTzBT-14HD/$PC_{61}BM$ thin films tended to adopt the face-on orientation when the MWs of PTzBT-14HD increased from 13 kg mol^{-1} to 73 kg mol^{-1} (Fig. 2e–h), leading to an increased J_{sc} from 6.1 mA cm^{-2} to 10.6 mA cm^{-2} and thus an enhanced PCE from 3.1% to 5.7% as a result of the preferred hole transport along the face-on orientation toward the anode.[83] Notably, the crystallinity was slightly decreased at the very high MW of 73 kg mol^{-1}, which was probably induced by the increased structural disorder or the reduced crystallization kinetics due to extremely long polymer chains.

2.2 Extending π conjugation of backbones

The self-assembly and optoelectronic properties of LBG polymers are relied strongly on the π–π interactions of conjugated backbones.[86–88] The planarity of conjugated backbones directly impacts on the solubility, electronic levels, film morphology, and charge carrier mobility of CPs.[89] Extending the π-conjugation length of backbones has been proposed as an effective route to improving the optoelectronic properties of LBG polymers with better π-electron delocalization.[90,91] To this end, the π-conjugation extension has been achieved by incorporating rigid fused aromatic structures into the conjugated backbones or reducing the steric hindrance between adjacent backbones.[92–94]

A representative example is the recently reported molecular modification of a LBG polymer, poly[(2-((2-ethylhexyl)sulfonyl)-thieno[3,-*b*]thiophen-2,6-diyl)-*alt*-(4,8-bis(2-ethylhexyloxy)benzo-[1,2-*b*:4,5-*b*′]dithiophene)-2,6-diyl] (PBDTTT-S), which comprises

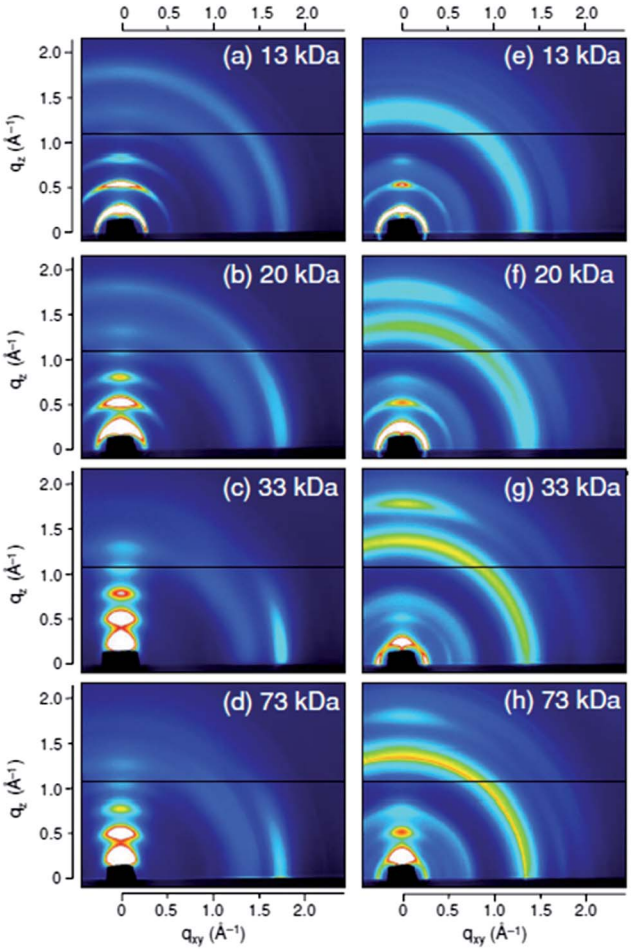

Fig. 2 (a–d) 2D grazing incidence wide angle X-ray diffraction (GIWXRD) patterns of the PTzBT-14HD thin films with different molecular weights. (e–h) 2D GIWXRD patterns of the PTzBT-14HD/$PC_{61}BM$ blend thin films with different molecular weights of PTzBT-14HDs.[83] Adapted with permission from ref. 83, Copyright© 2012 Wiley-VCH.

benzo[1,2-*b*:4,5-*b*′]dithiophene (BDT) and thieno[3,4-*b*]thiophene (TT) units. When mixing with $PC_{71}BM$, PBDTTT-S exhibited a high V_{oc} of 0.76 V, yet a relatively low J_{sc} of 13.8 mA cm^{-2} and a FF of 58.0%.[95] The density functional theory (DFT) calculations suggested that the large sulfonyl bond angle (*i.e.*, ~108°) between the BDT and TT units was unfavorable for π–π stacking of PBDTTT-S.[95] Excessive backbone twisting can increase the optical bandgap and decrease the hole mobility of CPs, which was probably responsible for the relatively low J_{sc} and FF in PBDTTT-S.[96] In order to improve the π conjugation, thienyl units were introduced into the BDT side chain to increase the conjugated area (*i.e.*, both along the backbone and the side chain). The thienyl units were also introduced between the BDT and TT units to decrease the torsional angle and thus reduce the steric hindrance for π–π stacking (Fig. 3a).[95,97,98] The resulting LBG polymer PBDTDTTT-S-T displayed a markedly enhanced crystallinity, and adopted a mixed edge-on and face-on orientation with a decreased π–π stacking distance of 3.51 Å as compared to that of 3.88 Å in PBDTTT-S thin films.[95] Moreover, PBDTDTTT-S-T nanowires appeared in the PBDTDTTT-S-T/$PC_{71}BM$ blend thin films. These nanowires were well-mixed with $PC_{71}BM$ molecules (Fig. 3b and c), leading to an increased hole mobility from 4.56 × 10^{-4} cm^2 V^{-1} s^{-1} (*i.e.*, PBDTTT-S/$PC_{71}BM$) to 2.76 × 10^{-3} cm^2 V^{-1} s^{-1} (*i.e.*, PBDTDTTT-S-T/$PC_{71}BM$), a J_{sc} from 13.85 mA cm^{-2} to 16.35 mA cm^{-2} and a FF from 58.0% to 66.3%. Consequently, the highest EQE of PBDTTT-S-T-based solar cells exceeded 70% (Fig. 3d), and the PCE reached 7.48%.[95]

2.3 Varying alkyl-side chains

The introduction of alkyl side chains on CPs is primarily expected to increase the solubility of rigid CP backbones in organic solvents,[31,99–101] thereby facilitating their solution-based synthesis and processing. Depending on the interchain interaction between alkyl side chains and conjugated backbones, the

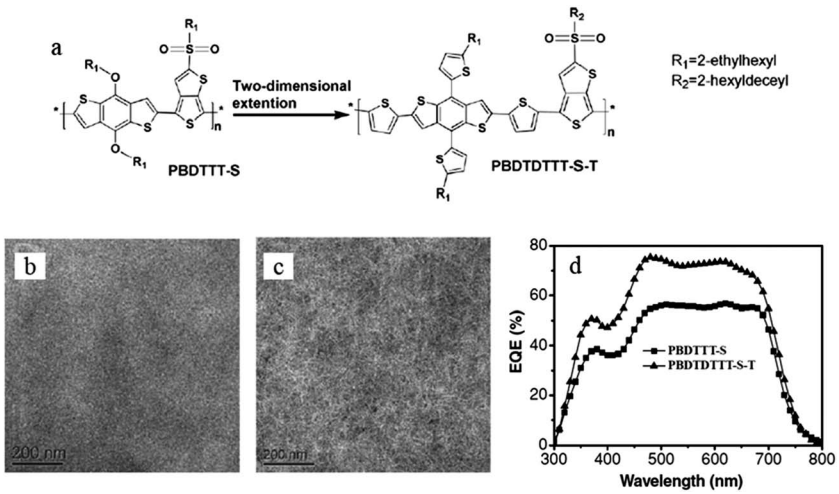

Fig. 3 (a) Molecular structures of PBDTTT-S and PBDTDTTT-S-T. (b) TEM image of the PBDTTT-S/$PC_{71}BM$ (1 : 1.5, w/w) blend thin film. (c) TEM image of the PBDTTT-S-T/$PC_{71}BM$ (1 : 1, w/w) blend thin film. (d) External quantum efficiency (EQE) of PBDTTT-S/$PC_{71}BM$- and PBDTTT-S-T/$PC_{71}BM$-based solar cells.[95] Adapted with permission from ref. 95, Copyright© 2012 Wiley-VCH.

solubility, self-assembly, charge intensity, energy level, and film morphology of CPs are varied with the incorporation of different alkyl side chains.[102–105] In principle, the alkyl side chains should be employed as solubilizing substituents in a manner that the π–π stacking of conjugated backbones is not largely hindered by coil-like alkyl chains and the electronic properties of CPs is not heavily reduced by the insulating nature of alkyl chains.[106] Moreover, the introduction of alkyl side chains is beneficial for improving the miscibility of CPs with fullerenes within the BHJ blend films.[107] Therefore, it is of particular importance to optimize the use of alkyl side chains, such as the choice of branching position as well as alkyl composition, length, topology (*e.g.*, linear, branched) and density. Recently, a well-organized poly(3-alkylthiophene) (P3AT)-based BHJ nanostructure was achieved in poly-(3-butylthiophene)-*b*-poly(3-hexylthiophene)/$PC_{71}BM$ solar cells by tuning the ratio of butyl- and hexyl-side chains on the conjugated thienyl backbones.[108] The as-prepared finer BHJ nanostructures were composed of (1) small P3AT crystalline domains (*i.e.*, ~10 nm) that were comparable to the exciton diffusion length of P3ATs, (2) microphase-separated P3AT/$PC_{71}BM$ that provided large-area donor–acceptor interfaces, and (3) interpenetrating P3AT crystalline networks for the effective hole transport, leading to an attractive PCE of 4.02% compared to that of ~3.15% in P3HT/$PC_{71}BM$ blends.

For LBG polymers, the influences of alkyl side chains on their molecular conformation, self-assembly, energy level, and film morphology are more complicated than those of CP homopolymers with relatively simple molecular structures.[21,109] The complex molecular structures of LBG polymers offer expanded flexibility for optimizing the film morphology and optoelectronic properties of LBG polymers by varying the alkyl side chains. Recently, it has been demonstrated that the linear alkyl side chains rendered a better balance between the solubility and molecular ordering than the branched alkyl side chains in the DPP-based LBG polymer PDPP2FT (Fig. 1e).[110] The interdigitation of linear alkyl chains probably facilitated the lamellar packing of PDPP2FT and in turn promoted the π–π stacking of PDPP2FT backbones,[106] resulting in an enhanced PCE from ~5% (*i.e.*, branched-alkyl-substituted PDPP2FT) to 6.5%. The incorporation of linear alkyl side chains situated on the proper positions of conjugated backbones may not only increase the solubility but also induce an orientational transformation from the edge-on to face-on orientation, leading to an enhanced hole transport toward the anode and thus high PCEs.[111]

We note that the effects of linear and branched alkyl side chains on molecular orientation of LBG polymers have been systematically studied in the thiophene–thiazolothiazole copolymer PTzBT by varying the lengths of linear and branched alkyl side chains.[112] The molecular orientation of PTzBT thin films can be controlled by adjusting the lengths of adjacent alkyl side chains on the backbones (*i.e.*, R^1 and R^2 in Fig. 4). For the linear-branched case (*i.e.*, R^1 = linear alkyl side chains and R^2 = branched alkyl side chains), a shorter linear alkyl side chain was preferred for the face-on orientation; while in the all-branched (*i.e.*, R^1 and R^2 = branched alkyl side chains) case, a small length difference between R^1 and R^2 was preferred for

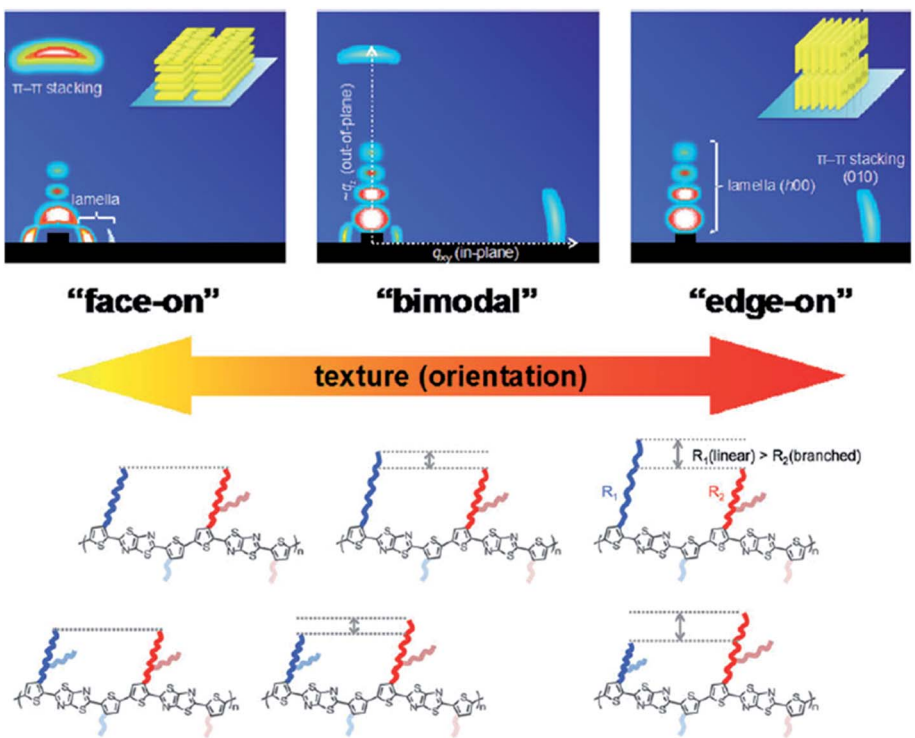

Fig. 4 Schematic illustration of the molecular orientation of PTzBT thin films based on the different lengths of alkyl side chains.[112] Adapted with permission from ref. 112, Copyright© 2013 Wiley-VCH.

the face-on orientation.[112] Hence, the intermolecular interactions between the alkyl side chains and conjugated backbones governed the molecular orientation of LBG polymer thin films.[113,114] It is noteworthy that only the face-on orientation was observed in the PTzBT/$PC_{61}BM$ blend thin films,[112] regardless of the compositions of alkyl side chains. This suggested that the π–π interactions between the conjugated backbones and fullerenes dominated the molecular orientation in polymer/fullerene blend films.[115]

The intramolecular interactions between alkyl side chains and conjugated backbones influence the molecular coplanarity, and in turn change the solubility, molecular orientation, and film morphology of LBG polymers. Recently, a series of alkyl side chains (*i.e.*, 2-ethylhexyl, decyl, dodecyl) with different sizes and topologies were incorporated into the thienyl side units of PBDT-T-TPD. The DFT calculations inferred that the PBDT-T8-TPD with 2-ethylhexyl side chains held the worst planarity, the PBDT-T12-TPD with dodecyl side chains had a better planarity, and the PBDT-T10-TPD with decyl side chains possessed the best planarity (Fig. 5),[116] correlating well with the PCEs of 2.16%, 3.14%, and 4.15% for PBDT-T8-TPD/$PC_{61}BM$, PBDT-T12-TPD/$PC_{61}BM$, and PBDT-T10-TPD/$PC_{61}BM$ solar cells without any additives, respectively. The correlation between the polymer coplanarity and PCE signified the importance of polymer coplanarity on the light absorption, charge transport, film morphology, and thus the photovoltaic characteristics (*i.e.*, J_{sc} and FF). For example, the PBDT-T8-TPD with the worst planarity displayed the lowest J_{sc}, FF and PCE (Table 1).[116] More interestingly, the PCE of PBDT-T8-TPD/$PC_{61}BM$ solar cells was dramatically raised to 6.17% with an increased FF and J_{sc} after the addition of 1,8-diiodooctane (DIO) as the solvent additive, indicating that the miscibility and intermolecular interactions between PBDT-T8-TPD and $PC_{61}BM$ were greatly improved by the solvent additive, due probably to the more flexible and soluble nature of PBDT-T8-TPD chains.[116]

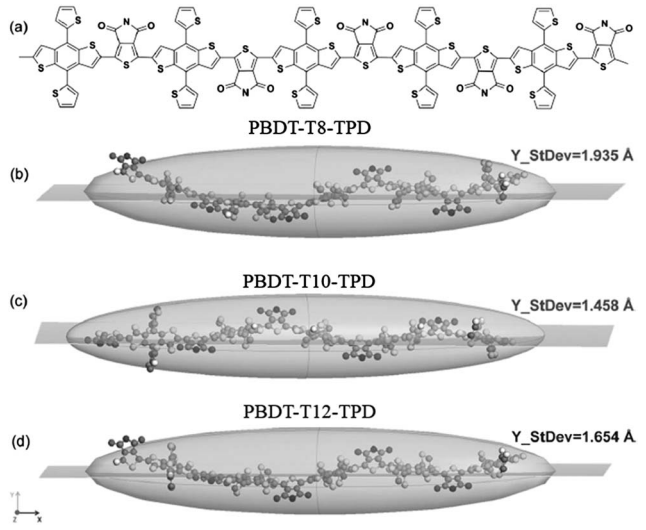

Fig. 5 (a) Schematic illustration of the backbone structure of pentamers of PBDT-T-TPD with different alkyl side chains. The alkyl side chains are located at the thienyl side units. (b–d) The calculated steric arrangement of backbones for PBDT-T8-TPD, PBDT-T10-TPD and PBDT-T12-TPD, respectively. The ellipsoids represent the approximate shape of pentamers. Y_StDev is defined as the calculated standard deviations of Y coordinates of each atom.[116] Adapted with permission from ref. 116, Copyright© 2013 Wiley-VCH.

Table 1 Photovoltaic properties of LBG polymer-based solar cells based on PBDT-T-TPD and PBDT-TPD under the illumination of AM1.5G, 100 mW cm^{-2}. CF and DIO represent chloroform and 1,8-diiodooctane, respectively.[116] Adapted with permission from ref. 116, Copyright© 2012 Wiley-VCH

Polymer	Solvent	J_{sc} [mA cm^{-2}]	V_{oc} [V]	FF [%]	PCE [%]
PBDT-T8-TPD	CF	5.90	0.96	38.1	2.16
PBDT-T8-TPD	CF + 3% DIO	9.79	1.00	63.0	6.17
PBDT-T10-TPD	CF	8.18	0.92	55.1	4.15
PBDT-T10-TPD	CF + 3% DIO	8.92	0.92	55.0	4.51
PBDT-T12-TPD	CF	6.69	0.96	49.0	3.14
PBDT-T12-TPD	CF + 3% DIO	8.94	0.95	53.2	4.50
PBDT-TPD	CF	8.63	0.85	47.5	3.48
PBDT-TPD	CF + 2% DIO	10.74	0.90	49.4	4.77

3. Nanomorphology evolution with solvent additives

Thermal- and solvent-annealing treatments have been recognized as the most effective post-treatment procedures for improving the efficiency of P3HT-based BHJ solar cells,[117–120] which are mainly attributed to the enhanced P3HT crystallization and better developed microphase separation between P3HT and fullerenes.[63] However, these post-treatments are no longer effective for most LBG polymer-based solar cells. The device degradations are usually observed with the increase in thermal-annealing temperature or solvent-annealing time due to the aggregation of fullerene molecules or the reduction of π–π stacking coherence of LBG polymers.[121,122] However, the use of solvent additives such as DIO, 1-chloronaphthalene (CN), and 1,8-octanedithiol (ODT) can markedly improve the BHJ morphology of LBG polymer-based solar cells, leading to significantly enhanced performance.[64,123,124]

Although the underlying mechanism of solvent additive-enhanced photovoltaic performance is still under investigation, the criteria for optimizing the film morphology of LBG polymer-based solar cells using solvent additives are suggested as follows: (1) the additive must have a higher boiling point than the host solvent; (2) the additive should possess selective solubility on one of the two components in the BHJ blend; (3) the molecular order of LBG polymers may be promoted by solvent additives; and (4) the miscibility of LBG polymer and fullerene molecules may be improved by solvent additives.[125,126] In addition, the use of binary additives (*e.g.*, DIO–CN mixture) may work more effectively for improving the film morphology through controlling the nanomorphology evolution of LBG polymers and fullerenes.[127,128] Recent advance in GIWAXD, GISAXS, and RSoXS renders the time-resolved characterization of nanomorphology evolution of LBG polymer-based solar cells

during the film-forming process,[51] which is advantageous as it provides a better understanding of the kinetics of solvent additive-processed BHJ nanostructure formation and offers a rational pathway toward the optimization of LBG polymer-based solar cells.

In contrast to the semicrystalline nature of P3HT, most LBG polymers have very low crystallinity, and even seem amorphous.[129,130] However, the formation of interconnected nanoaggregates within the LBG polymer domains improves the short-range order, which is sufficiently pervasive in the thin-film microstructures to provide an effective pathway for charge transport and thus high optoelectronic properties.[78] Compared to the BHJ nanostructure of P3HT/fullerene solar cells, LBG polymer/fullerene thin films may possess more complex hierarchical BHJ nanomorphology, thus imparting an enhanced exciton dissociation, charge generation, and charge transport.[131] For example, a multi-length-scale hierarchical BHJ morphology was found to exist in the photoactive layer of $PTB_7/PC_{61}BM$ solar cells, which contained (1) randomly dispersed PTB7 (Fig. 1f) chains and $PC_{61}BM$ at the molecular level, (2) nanocrystalline $PTB7/PC_{61}BM$ aggregates within PTB7-rich and fullerene-rich domains, and (3) microphase-separated $PTB7/PC_{61}BM$ domains (Fig. 6).[131]

The development of the multi-length-scale morphology is largely dictated by the kinetic nature and the role of different components during the film-forming process. Notably, the solubilities of LBG polymer and fullerene in the processing solution act as the driving force for the aggregations of the LBG polymer and fullerene at different stages of the film-forming process, responsible for the evolution of hierarchical morphology of the LBG polymer/fullerene photoactive layer. For example, for the $PTB7/PC_{61}BM$ blend, the host solvent chlorobenzene (CB) is a good solvent for both PTB7 and $PC_{61}BM$; the additive DIO is a good solvent for $PC_{61}BM$ but a poor solvent for PTB7. The addition of DIO promoted the aggregation of PTB7 at the early stage of the film-drying process while preventing the formation of large sized $PC_{61}BM$ aggregates.[132] This led to the finer hierarchical morphology with improved efficiency. Similar additive effects on promoting the formation of multi-length-scale morphology for enhanced exciton dissociation and charge transport were also observed in $PBDTP\text{-}DTBT/PC_{71}CM$ solar cells (Fig. 1g) using DIO as the solvent additive and in $PDPP2FT/PC_{61}BM$ solar cells using CN as the solvent additive.[133,134] We note that the fundamental relationship between the solvent additive and the nanomorphology of LBG polymer-based solar cells is still under exploration. A comprehensive understanding of the short-range order, the interpenetrating charge transport, and the hierarchical structure in LBG polymer-based solar cells is the key to yielding high performance polymer solar cells.

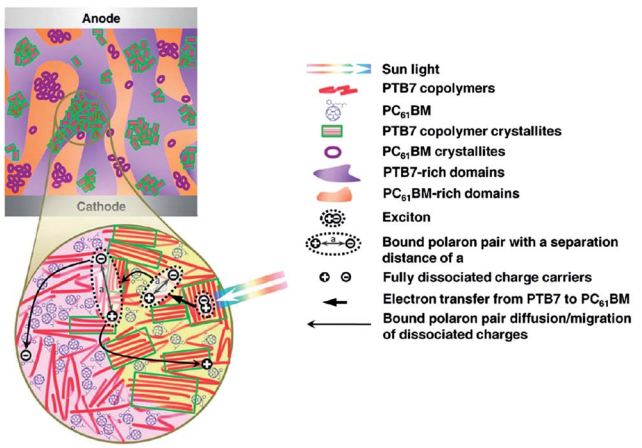

Fig. 6 Schematic illustration of the hierarchical BHJ morphology for $PTB7/PC_{61}BM$ solar cells.[131] Adapted with permission from ref. 131, Copyright© 2011 American Chemical Society.

4. Conclusions and outlook

The past few years have been witness to rapid advances in rational design and synthesis of "push–pull" LBG polymers with tailored HOMO and LUMO levels for high V_{oc}, fast charge carrier mobility, and enhanced optical absorption, and thus significantly improved performance of polymer solar cells. The highest PCE of LBG polymer-based solar cells has exceeded 10% with optimized energy levels and device architectures.[37,135,136] Owing to the complex non-covalent interchain interactions (*e.g.*, π–π interaction, hydrogen-bond interaction, and van der Waals forces) of electron-donating and electron-withdrawing units,[67] the chemical structure of LBG polymers impacts not only the intrinsic optoelectronic properties, but also the film morphology of the resulting solar cells. Several strategies for optimizing the film morphology of LBG polymer-based solar cells have been successfully employed: (1) increasing the molecular weight of LBG polymers to provide better connections between ordered regions for efficient charge transport; (2) extending the π–π conjugation length of backbones to facilitate the π-electron delocalization for a smaller band gap of LBG polymers; and (3) varying the composition, length, topology, density, and position of alkyl side chains for finer nanostructures. In addition to the molecular engineering, the use of solvent additives has been proven as the most effective route to optimizing the film morphology. A variety of *in situ* characterization techniques (*e.g.*, GIWAXD, GISAXS, RSoXS, *etc.*) have been applied to analyze the morphology evolution of LBG polymer-based solar cells with solvent additives, thereby offering a better understanding on the kinetics of additive-processed nanostructure formation.

Despite the exciting efficiency of over 10%, further exploration on the molecular design, morphology optimization, and thorough fundamental understanding of optoelectronic behaviors of LBG polymers are still required for improved efficiency and stability of polymer solar cells. This includes (1) the design of new LBG polymers with the broadened absorption spectra to increase the light harvesting efficiency; (2) the investigation of the relationship between the multi-length-scale hierarchical morphology and optoelectronic properties of LBG polymers to provide enabling strategies for optimized polymer solar cells; (3) the ability to tune the interfacial energy alignment between LBG polymer/fullerene photoactive layers and electrodes to increase the charge collection efficiency of LBG polymer-based solar cells; and (4) the synthesis of novel organic

or inorganic semiconductors as acceptors to replace the expensive fullerene materials; and (5) the construction of intimate contact between LBG polymer donors and inorganic acceptors to develop high efficiency organic–inorganic hybrid solar cells.[137] Nonetheless, with the progress being made in the synthesis of LBG polymers, further understanding of molecular organization and nanoscale morphology, device engineering and optimization, LBG polymer-based solar cells will have a bright and rapidly evolving future for the practical organic photovoltaic cells with the ease of handling, high performance, low cost, and long term stability.

Acknowledgements

We gratefully acknowledge funding support from the Air Force Office of Scientific Research (FA9550-13-1-0101), National Science Foundation (ECCS-1305087) and Minjiang Scholar Program. M.W. gratefully acknowledges the financial support from the Chinese Scholarship Council (CSC).

References

1 W. U. Huynh, J. J. Dittmer and A. P. Alivisatos, *Science*, 2002, **295**, 2425.
2 J. Y. Kim, K. Lee, N. E. Coates, D. Moses, T. Q. Nguyen, M. Dante and A. J. Heeger, *Science*, 2007, **317**, 222.
3 M. Graetzel, R. A. J. Janssen, D. B. Mitzi and E. H. Sargent, *Nature*, 2012, **488**, 304.
4 C. J. Brabec, N. S. Sariciftci and J. C. Hummelen, *Adv. Funct. Mater.*, 2001, **11**, 15.
5 S. Gunes, H. Neugebauer and N. S. Sariciftci, *Chem. Rev.*, 2007, **107**, 1324.
6 Y. Y. Liang, Z. Xu, J. B. Xia, S. T. Tsai, Y. Wu, G. Li, C. Ray and L. P. Yu, *Adv. Mater.*, 2010, **22**, E135.
7 F. C. Krebs, S. A. Gevorgyan and J. Alstrup, *J. Mater. Chem.*, 2009, **19**, 5442.
8 G. Li, V. Shrotriya, J. S. Huang, Y. Yao, T. Moriarty, K. Emery and Y. Yang, *Nat. Mater.*, 2005, **4**, 864.
9 A. Marrocchi, D. Lanari, A. Facchetti and L. Vaccaro, *Energy Environ. Sci.*, 2012, **5**, 8457.
10 M. He, L. Zhao, J. Wang, W. Han, Y. L. Yang, F. Qiu and Z. Q. Lin, *ACS Nano*, 2010, **4**, 3241.
11 M. He, F. Qiu and Z. Q. Lin, *J. Mater. Chem.*, 2011, **21**, 17039.
12 M. He, J. Ge, M. Fang, F. Qiu and Y. L. Yang, *Polymer*, 2010, **51**, 2236.
13 P. M. Allemand, A. Koch, F. Wudl, Y. Rubin, F. Diederich, M. M. Alvarez, S. J. Anz and R. L. Whetten, *J. Am. Chem. Soc.*, 1991, **113**, 1050.
14 T. B. Singh, N. Marjanovic, G. J. Matt, S. Gunes, N. S. Sariciftci, A. M. Ramil, A. Andreev, H. Sitter, R. Schwodiauer and S. Bauer, *Org. Electron.*, 2005, **6**, 105.
15 A. J. Moule, L. L. Chang, C. Thambidurai, R. Vidu and P. Stroeve, *J. Mater. Chem.*, 2012, **22**, 2351.
16 S. Nizamoglu, X. W. Sun and H. V. Demir, *Appl. Phys. Lett.*, 2010, **97**, 263106.
17 J. L. Birman and N. Q. Huong, *J. Lumin.*, 2007, **125**, 196.
18 M. R. Narayan and J. Singh, *J. Appl. Phys.*, 2013, **114**, 073510.
19 H. Y. Chen, J. H. Hou, S. Q. Zhang, Y. Y. Liang, G. W. Yang, Y. Yang, L. P. Yu, Y. Wu and G. Li, *Nat. Photonics*, 2009, **3**, 649.
20 G. Dennler, M. C. Scharber and C. J. Brabec, *Adv. Mater.*, 2009, **21**, 1323.
21 N. Blouin, A. Michaud, D. Gendron, S. Wakim, E. Blair, R. Neagu-Plesu, M. Belletete, G. Durocher, Y. Tao and M. Leclerc, *J. Am. Chem. Soc.*, 2008, **130**, 732.
22 M. C. Scharber, D. Wuhlbacher, M. Koppe, P. Denk, C. Waldauf, A. J. Heeger and C. L. Brabec, *Adv. Mater.*, 2006, **18**, 789.
23 J. L. Li and A. C. Grimsdale, *Chem. Soc. Rev.*, 2010, **39**, 2399.
24 L. Beverina and G. A. Pagani, *Acc. Chem. Res.*, 2013, DOI: 10.1021/ar4000967.
25 J. W. Chen and Y. Cao, *Acc. Chem. Res.*, 2009, **42**, 1709.
26 R. S. Kularatne, H. D. Magurudeniya, P. Sista, M. C. Biewer and M. C. Stefan, *J. Polym. Sci., Part A: Polym. Chem.*, 2013, **51**, 743.
27 S. C. Rasmussen, R. L. Schwiderski and M. E. Mulholland, *Chem. Commun.*, 2011, **47**, 11394.
28 Y. F. Li, *Acc. Chem. Res.*, 2012, **45**, 723.
29 H. H. Chang, C. E. Tsai, Y. Y. Lai, D. Y. Chiou, S. L. Hsu, C. S. Hsu and Y. J. Cheng, *Macromolecules*, 2012, **45**, 9282.
30 Y. Y. Liang, D. Q. Feng, Y. Wu, S. T. Tsai, G. Li, C. Ray and L. P. Yu, *J. Am. Chem. Soc.*, 2009, **131**, 7792.
31 T. Y. Chu, J. P. Lu, S. Beaupre, Y. G. Zhang, J. R. Pouliot, S. Wakim, J. Y. Zhou, M. Leclerc, Z. Li, J. F. Ding and Y. Tao, *J. Am. Chem. Soc.*, 2011, **133**, 4250.
32 L. J. Huo, J. H. Hou, S. Q. Zhang, H. Y. Chen and Y. Yang, *Angew. Chem., Int. Ed.*, 2010, **49**, 1500.
33 H. X. Zhou, L. Q. Yang, S. C. Price, K. J. Knight and W. You, *Angew. Chem., Int. Ed.*, 2010, **49**, 7992.
34 A. Bhuwalka, J. F. Mike, M. He, J. J. Intemann, T. Nelson, M. D. Ewan, R. A. Roggers, Z. Q. Lin and M. Jeffries-El, *Macromolecules*, 2011, **44**, 9611.
35 H. X. Zhou, L. Q. Yang, A. C. Stuart, S. C. Price, S. B. Liu and W. You, *Angew. Chem., Int. Ed.*, 2011, **50**, 2995.
36 J. H. Hou, Z. A. Tan, Y. Yan, Y. J. He, C. H. Yang and Y. F. Li, *J. Am. Chem. Soc.*, 2006, **128**, 4911.
37 J. B. You, L. T. Dou, K. Yoshimura, T. Kato, K. Ohya, T. Moriarty, K. Emery, C. C. Chen, J. Gao, G. Li and Y. Yang, *Nat. Commun.*, 2013, **4**, 1446.
38 J. Nelson, *Curr. Opin. Solid State Mater. Sci.*, 2002, **6**, 87.
39 N. S. Sariciftci, D. Braun, C. Zhang, V. I. Srdanov, A. J. Heeger, G. Stucky and F. Wudl, *Appl. Phys. Lett.*, 1993, **62**, 585.
40 G. Yu and A. J. Heeger, *J. Appl. Phys.*, 1995, **78**, 4510.
41 P. W. M. Blom, V. D. Mihailetchi, L. J. A. Koster and D. E. Markov, *Adv. Mater.*, 2007, **19**, 1551.
42 J. Jo, S. I. Na, S. S. Kim, T. W. Lee, Y. Chung, S. J. Kang, D. Vak and D. Y. Kim, *Adv. Funct. Mater.*, 2009, **19**, 2398.
43 S. R. Cowan, A. Roy and A. J. Heeger, *Phys. Rev. B: Condens. Matter Mater. Phys.*, 2010, **82**, 245207.
44 A. A. Bakulin, A. Rao, V. G. Pavelyev, P. H. M. van Loosdrecht, M. S. Pshenichnikov, D. Niedzialek, J. Cornil, D. Beljonne and R. H. Friend, *Science*, 2012, **335**, 1340.
45 P. M. Beaujuge and J. M. J. Frechet, *J. Am. Chem. Soc.*, 2011, **133**, 20009.

46 M. O'Neill and S. M. Kelly, *Adv. Mater.*, 2011, **23**, 566.
47 E. Cho, C. Risko, D. Kim, R. Gysel, N. C. Miller, D. W. Breiby, M. D. McGehee, M. F. Toney, R. J. Kline and J. L. Bredas, *J. Am. Chem. Soc.*, 2012, **134**, 6177.
48 A. A. Herzing, H. W. Ro, C. L. Soles and D. M. Delongchamp, *ACS Nano*, 2013, **7**, 7937.
49 M. C. Shih, B. C. Huang, C. C. Lin, S. S. Li, H. A. Chen, Y. P. Chiu and C. W. Chen, *Nano Lett.*, 2013, **13**, 2387.
50 W. Yin and M. Dadmun, *ACS Nano*, 2011, **5**, 4756.
51 F. Liu, Y. Gu, X. B. Shen, S. Ferdous, H. W. Wang and T. P. Russell, *Prog. Polym. Sci.*, 2013, **38**, 1990.
52 W. Chen, M. P. Nikiforov and S. B. Darling, *Energy Environ. Sci.*, 2012, **5**, 8045.
53 J. Rivnay, S. C. B. Mannsfeld, C. E. Miller, A. Salleo and M. F. Toney, *Chem. Rev.*, 2012, **112**, 5488.
54 B. J. de Gans, S. Wiegand, E. R. Zubarev and S. I. Stupp, *J. Phys. Chem. B*, 2002, **106**, 9730.
55 T. Wang, A. J. Pearson, D. G. Lidzey and R. A. L. Jones, *Adv. Funct. Mater.*, 2011, **21**, 1383.
56 D. A. Chen, A. Nakahara, D. G. Wei, D. Nordlund and T. P. Russell, *Nano Lett.*, 2011, **11**, 561.
57 M. S. Su, C. Y. Kuo, M. C. Yuan, U. S. Jeng, C. J. Su and K. H. Wei, *Adv. Mater.*, 2011, **23**, 3315.
58 W. R. Wu, U. S. Jeng, C. J. Su, K. H. Wei, M. S. Su, M. Y. Chiu, C. Y. Chen, W. B. Su, C. H. Su and A. C. Su, *ACS Nano*, 2011, **5**, 6233.
59 M. He, W. Han, J. Ge, W. J. Yu, Y. L. Yang, F. Qiu and Z. Q. Lin, *Nanoscale*, 2011, **3**, 3159.
60 G. Li, V. Shrotriya, Y. Yao and Y. Yang, *J. Appl. Phys.*, 2005, **98**, 043704.
61 E. Verploegen, R. Mondal, C. J. Bettinger, S. Sok, M. F. Toney and Z. A. Bao, *Adv. Funct. Mater.*, 2010, **20**, 3519.
62 G. Li, Y. Yao, H. Yang, V. Shrotriya, G. Yang and Y. Yang, *Adv. Funct.Mater.*, 2007, **17**, 1636.
63 L. H. Nguyen, H. Hoppe, T. Erb, S. Gunes, G. Gobsch and N. S. Sariciftci, *Adv. Funct. Mater.*, 2007, **17**, 1071.
64 F. Etzold, I. A. Howard, N. Forler, D. M. Cho, M. Meister, H. Mangold, J. Shu, M. R. Hansen, K. Mullen and F. Laquai, *J. Am. Chem. Soc.*, 2012, **134**, 10569.
65 J. Jo, A. Pron, P. Berrouard, W. L. Leong, J. D. Yuen, J. S. Moon, M. Leclerc and A. J. Heeger, *Adv. Energy Mater.*, 2012, **2**, 1397.
66 B. G. Kim, E. J. Jeong, J. W. Chung, S. Seo, B. Koo and J. S. Kim, *Nat. Mater.*, 2013, **12**, 659.
67 J. F. Jheng, Y. Y. Lai, J. S. Wu, Y. H. Chao, C. L. Wang and C. S. Hsu, *Adv. Mater.*, 2013, **25**, 2445.
68 B. C. Thompson and J. M. J. Frechet, *Angew. Chem., Int. Ed.*, 2008, **47**, 58.
69 C. J. Brabec, M. Heeney, I. McCulloch and J. Nelson, *Chem. Soc. Rev.*, 2011, **40**, 1185.
70 M. T. Dang, L. Hirsch, G. Wantz and J. D. Wuest, *Chem. Rev.*, 2013, **113**, 3734.
71 F. Liu, Y. Gu, J. W. Jung, W. H. Jo and T. P. Russell, *J. Polym. Sci., Part B: Polym. Phys.*, 2012, **50**, 1018.
72 J. Peet, A. J. Heeger and G. C. Bazan, *Acc. Chem. Res.*, 2009, **42**, 1700.
73 J. Ge, M. He, X. B. Yang, Z. Ye, X. F. Liu and F. Qiu, *J. Mater. Chem.*, 2012, **22**, 19213.
74 H. J. Son, B. Carsten, I. H. Jung and L. P. Yu, *Energy Environ. Sci.*, 2012, **5**, 8158.
75 R. J. Kline, M. D. McGehee, E. N. Kadnikova, J. S. Liu, J. M. J. Frechet and M. F. Toney, *Macromolecules*, 2005, **38**, 3312.
76 A. Zen, J. Pflaum, S. Hirschmann, W. Zhuang, F. Jaiser, U. Asawapirom, J. P. Rabe, U. Scherf and D. Neher, *Adv. Funct. Mater.*, 2004, **14**, 757.
77 R. J. Kline, M. D. McGehee, E. N. Kadnikova, J. S. Liu and J. M. J. Frechet, *Adv. Mater.*, 2003, **15**, 1519.
78 R. Noriega, J. Rivnay, K. Vandewal, F. P. V. Koch, N. Stingelin, P. Smith, M. F. Toney and A. Salleo, *Nat. Mater.*, 2013, **12**, 1038.
79 S. Y. Qu and H. Tian, *Chem. Commun.*, 2012, **48**, 3039.
80 J. C. Bijleveld, V. S. Gevaerts, D. Di Nuzzo, M. Turbiez, S. G. J. Mathijssen, D. M. de Leeuw, M. M. Wienk and R. A. J. Janssen, *Adv. Mater.*, 2010, **22**, E242.
81 K. H. Hendriks, G. H. L. Heintges, V. S. Gevaerts, M. M. Wienk and R. A. J. Janssen, *Angew. Chem., Int. Ed.*, 2013, **52**, 8341.
82 W. W. Li, K. H. Hendriks, W. S. C. Roelofs, Y. Kim, M. M. Wienk and R. A. J. Janssen, *Adv. Mater.*, 2013, **25**, 3182.
83 I. Osaka, M. Saito, H. Mori, T. Koganezawa and K. Takimiya, *Adv. Mater.*, 2012, **24**, 425.
84 I. Osaka, R. Zhang, G. Sauve, D. M. Smilgies, T. Kowalewski and R. D. McCullough, *J. Am. Chem. Soc.*, 2009, **131**, 2521.
85 I. Osaka, R. Zhang, J. Y. Liu, D. M. Smilgies, T. Kowalewski and R. D. McCullough, *Chem. Mater.*, 2010, **22**, 4191.
86 J. H. Hou, M. H. Park, S. Q. Zhang, Y. Yao, L. M. Chen, J. H. Li and Y. Yang, *Macromolecules*, 2008, **41**, 6012.
87 W. Y. Wong, X. Z. Wang, Z. He, K. K. Chan, A. B. Djurisic, K. Y. Cheung, C. T. Yip, A. M. C. Ng, Y. Y. Xi, C. S. K. Mak and W. K. Chan, *J. Am. Chem. Soc.*, 2007, **129**, 14372.
88 S. M. Zhang, Y. L. Guo, H. J. Fan, Y. Liu, H. Y. Chen, G. W. Yang, X. W. Zhan, Y. Q. Liu, Y. F. Li and Y. Yang, *J. Polym. Sci., Part A: Polym. Chem.*, 2009, **47**, 5498.
89 R. Rieger, D. Beckmann, A. Mavrinskiy, M. Kastler and K. Mullen, *Chem. Mater.*, 2010, **22**, 5314.
90 G. C. Welch, R. C. Bakus, S. J. Teat and G. C. Bazan, *J. Am. Chem. Soc.*, 2013, **135**, 2298.
91 H. J. Son, L. Y. Lu, W. Chen, T. Xu, T. Y. Zheng, B. Carsten, J. Strzalka, S. B. Darling, L. X. Chen and L. P. Yu, *Adv. Mater.*, 2013, **25**, 838.
92 S. Q. Zhang, L. Ye, Q. Wang, Z. J. Li, X. Guo, L. J. Huo, H. L. Fan and J. H. Hou, *J. Phys. Chem. C*, 2013, **117**, 9550.
93 C. Piliego, T. W. Holcombe, J. D. Douglas, C. H. Woo, P. M. Beaujuge and J. M. J. Frechet, *J. Am. Chem. Soc.*, 2010, **132**, 7595.
94 M. C. Scharber, M. Koppe, J. Gao, F. Cordella, M. A. Loi, P. Denk, M. Morana, H. J. Egelhaaf, K. Forberich, G. Dennler, R. Gaudiana, D. Waller, Z. G. Zhu, X. B. Shi and C. J. Brabec, *Adv. Mater.*, 2010, **22**, 367.
95 Y. Huang, X. Guo, F. Liu, L. J. Huo, Y. N. Chen, T. P. Russell, C. C. Han, Y. F. Li and J. H. Hou, *Adv. Mater.*, 2012, **24**, 3383.

96 S. W. Ko, E. T. Hoke, L. Pandey, S. H. Hong, R. Mondal, C. Risko, Y. P. Yi, R. Noriega, M. D. McGehee, J. L. Bredas, A. Salleo and Z. A. Bao, *J. Am. Chem. Soc.*, 2012, **134**, 5222.
97 X. L. Feng, V. Marcon, W. Pisula, M. R. Hansen, J. Kirkpatrick, F. Grozema, D. Andrienko, K. Kremer and K. Mullen, *Nat. Mater.*, 2009, **8**, 421.
98 W. Pisula, Z. Tomovic, C. Simpson, M. Kastler, T. Pakula and K. Mullen, *Chem. Mater.*, 2005, **17**, 4296.
99 G. Q. Ren, P. T. Wu and S. A. Jenekhe, *Chem. Mater.*, 2010, **22**, 2020.
100 P. T. Wu, G. Q. Ren, C. X. Li, R. Mezzenga and S. A. Jenekhe, *Macromolecules*, 2009, **42**, 2317.
101 E. R. Zubarev, R. V. Talroze, T. I. Yuranova, N. A. Plate and H. Finkelmann, *Macromolecules*, 1998, **31**, 3566.
102 E. J. Zhou, C. He, Z. Tan, C. H. Yang and Y. F. Li, *J. Polym. Sci., Part A: Polym. Chem.*, 2006, **44**, 4916.
103 S. Miyanishi, K. Tajima and K. Hashimoto, *Macromolecules*, 2009, **42**, 1610.
104 J. G. Mei, D. H. Kim, A. L. Ayzner, M. F. Toney and Z. A. Bao, *J. Am. Chem. Soc.*, 2011, **133**, 20130.
105 Y. P. Zou, W. P. Wu, G. Y. Sang, Y. Yang, Y. Q. Liu and Y. F. Li, *Macromolecules*, 2007, **40**, 7231.
106 J. Ge, M. He, F. Qiu and Y. L. Yang, *Macromolecules*, 2010, **43**, 6422.
107 A. Gadisa, W. D. Oosterbaan, K. Vandewal, J. C. Bolsee, S. Bertho, J. D'Haen, L. Lutsen, D. Vanderzande and J. V. Manca, *Adv. Funct. Mater.*, 2009, **19**, 3300.
108 M. He, W. Han, J. Ge, Y. L. Yang, F. Qiu and Z. Q. Lin, *Energy Environ. Sci.*, 2011, **4**, 2894.
109 C. H. Duan, F. Huang and Y. Cao, *J. Mater. Chem.*, 2012, **22**, 10416.
110 A. T. Yiu, P. M. Beaujuge, O. P. Lee, C. H. Woo, M. F. Toney and J. M. J. Frechet, *J. Am. Chem. Soc.*, 2012, **134**, 2180.
111 I. Osaka, T. Kakara, N. Takemura, T. Koganezawa and K. Takimiya, *J. Am. Chem. Soc.*, 2013, **135**, 8834.
112 I. Osaka, M. Saito, T. Koganezawa and K. Takimiya, *Adv. Mater.*, 2014, **26**, 331.
113 J. S. Lee, S. K. Son, S. Song, H. Kim, D. R. Lee, K. Kim, M. J. Ko, D. H. Choi, B. Kim and J. H. Cho, *Chem. Mater.*, 2012, **24**, 1316.
114 R. Fitzner, E. Mena-Osteritz, A. Mishra, G. Schulz, E. Reinold, M. Weil, C. Korner, H. Ziehlke, C. Elschner, K. Leo, M. Riede, M. Pfeiffer, C. Uhrich and P. Bauerle, *J. Am. Chem. Soc.*, 2012, **134**, 11064.
115 Y. Kobori, R. Noji and S. Tsuganezawa, *J. Phys. Chem. C*, 2013, **117**, 1589.
116 J. Y. Yuan, Z. C. Zhai, H. L. Dong, J. Li, Z. Q. Jiang, Y. Y. Li and W. L. Ma, *Adv. Funct. Mater.*, 2013, **23**, 885.
117 W. L. Ma, C. Y. Yang, X. Gong, K. Lee and A. J. Heeger, *Adv. Funct. Mater.*, 2005, **15**, 1617.
118 V. D. Mihailetchi, H. X. Xie, B. de Boer, L. J. A. Koster and P. W. M. Blom, *Adv. Funct. Mater.*, 2006, **16**, 699.
119 H. W. Tang, G. H. Lu, L. G. Li, J. Li, Y. Z. Wang and X. N. Yang, *J. Mater. Chem.*, 2010, **20**, 683.
120 V. Shrotriya, Y. Yao, G. Li and Y. Yang, *Appl. Phys. Lett.*, 2006, **89**, 063505.
121 Z. M. Beiley, E. T. Hoke, R. Noriega, J. Dacuna, G. F. Burkhard, J. A. Bartelt, A. Salleo, M. F. Toney and M. D. McGehee, *Adv. Energy Mater.*, 2011, **1**, 954.
122 J. A. Bartelt, Z. M. Beiley, E. T. Hoke, W. R. Mateker, J. D. Douglas, B. A. Collins, J. R. Tumbleston, K. R. Graham, A. Amassian, H. Ade, J. M. J. Frechet, M. F. Toney and M. D. McGehee, *Adv. Energy Mater.*, 2013, **3**, 364.
123 L. T. Dou, J. Gao, E. Richard, J. B. You, C. C. Chen, K. C. Cha, Y. J. He, G. Li and Y. Yang, *J. Am. Chem. Soc.*, 2012, **134**, 10071.
124 S. P. Singh, C. H. P. Kumar, G. D. Sharma, J. A. Mikroyannidis, M. Singh and R. Kurchania, *J. Polym. Sci., Part B: Polym. Phys.*, 2012, **50**, 1612.
125 H. C. Liao, C. S. Tsao, Y. T. Shao, S. Y. Chang, Y. C. Huang, C. M. Chuang, T. H. Lin, C. Y. Chen, C. J. Su, U. S. Jeng, Y. F. Chen and W. F. Su, *Energy Environ. Sci.*, 2013, **6**, 1938.
126 Y. Kim, H. R. Yeom, J. Y. Kim and C. Yang, *Energy Environ. Sci.*, 2013, **6**, 1909.
127 D. H. Wang, A. K. K. Kyaw, J. R. Pouliot, M. Leclerc and A. J. Heeger, *Adv. Energy Mater.*, 2013, DOI: 10.1002/aenm.201300835.
128 B. R. Aich, J. P. Lu, S. Beaupre, M. Leclerc and Y. Tao, *Org. Electron.*, 2012, **13**, 1736.
129 S. Cho, J. H. Seo, S. H. Park, S. Beaupre, M. Leclerc and A. J. Heeger, *Adv. Mater.*, 2010, **22**, 1253.
130 X. H. Lu, H. Hlaing, D. S. Germack, J. Peet, W. H. Jo, D. Andrienko, K. Kremer and B. M. Ocko, *Nat. Commun.*, 2012, **3**, 795.
131 W. Chen, T. Xu, F. He, W. Wang, C. Wang, J. Strzalka, Y. Liu, J. G. Wen, D. J. Miller, J. H. Chen, K. L. Hong, L. P. Yu and S. B. Darling, *Nano Lett.*, 2011, **11**, 3707.
132 F. Liu, W. Zhao, J. R. Tumbleston, C. Wang, Y. Gu, D. Wang, A. L. Briseno, H. Ade and T. P. Russell, *Adv. Energy Mater.*, 2013, DOI: 10.1002/aenm.201301377.
133 M. J. Zhang, Y. Gu, X. Guo, F. Liu, S. Q. Zhang, L. J. Huo, T. P. Russell and J. H. Hou, *Adv. Mater.*, 2013, **25**, 4944.
134 K. Schmidt, C. J. Tassone, J. R. Niskala, A. T. Yiu, O. P. Lee, T. M. Weiss, C. Wang, J. M. J. Frechet, P. M. Beaujuge and M. F. Toney, *Adv. Mater.*, 2014, **26**, 300.
135 Z. C. He, C. M. Zhong, S. J. Su, M. Xu, H. B. Wu and Y. Cao, *Nat. Photonics*, 2012, **6**, 591.
136 J. You, C. C. Chen, Z. Hong, K. Yoshimura, K. Ohya, R. Xu, S. Ye, J. Gao, G. Li and Y. Yang, *Adv. Mater.*, 2013, **25**, 3973.
137 M. He, F. Qiu and Z. Q. Lin, *J. Phys. Chem. Lett.*, 2013, **4**, 1788.

